

The Critical Mass of Wilson Fermions: A Comparison of Perturbative and Monte Carlo Results

E. Follana and H. Panagopoulos

Department of Physics, University of Cyprus, P.O. Box 20537, Nicosia CY-1678, Cyprus

email: eduardo@dirac.ns.ucy.ac.cy, haris@ucy.ac.cy

(November 15, 2018)

Abstract

We calculate the critical value of the hopping parameter, κ_c , in Lattice QCD with Wilson fermions, to two loops in perturbation theory.

This quantity is an additive renormalization; as such, it is characterized not only by the standard caveats regarding the asymptotic nature of perturbative results, but also by a linear divergence in the lattice spacing. Consequently, our calculation tests rather stringently the limits of applicability of perturbation theory.

We compare our results to non perturbative evaluations of κ_c coming from Monte Carlo simulations.

Finally, we apply a tadpole improvement technique on our results; this shifts them quite favourably towards the non perturbative values.

Keywords: Lattice QCD, lattice renormalization, lattice perturbation theory, hopping parameter.

PACS numbers: 11.15.-q, 11.15.Ha, 12.38.G.

I. INTRODUCTION

In this paper we study the hopping parameter in lattice QCD with Wilson fermions. In particular, we compute its critical value to two loops in perturbation theory.

Wilson fermions are the most straightforward and widely used implementation of fermionic actions on the lattice. This implementation circumvents the fermion doubling problem by introducing a higher derivative term with a vanishing classical continuum limit, to lift unphysical propagator poles completely. At the same time, the action is strictly local, which is very advantageous for numerical simulation.

The price one pays for strict locality and absence of doublers is, of course, well known: The higher derivative term breaks chiral invariance explicitly. Thus, merely setting the bare fermionic mass to zero is not sufficient to ensure chiral symmetry in the quantum continuum limit; quantum corrections introduce an additive renormalization to the fermionic mass, which must then be fine tuned to have a vanishing renormalized value. Consequently, the hopping parameter κ , which is very simply related to the fermion mass, must be appropriately shifted from its naive value, to recover chiral invariance.

By dimensional power counting, the additive mass renormalization is seen to be linearly divergent with the lattice spacing. This adverse feature of Wilson fermions poses an additional problem to a perturbative treatment, aside from the usual issues related to lack of Borel summability. Indeed, our calculation serves as a check on the limits of applicability of perturbation theory, by comparison with non perturbative results coming from Monte Carlo simulations.

Starting from our two-loop results, we also provide improved estimates of the critical value of κ , by performing a resummation to all orders of cactus diagrams [1]. These are tadpole-like diagrams which are gauge invariant and dress the propagators and vertices in our calculation. This improvement technique, among others, has so far been applied mostly to the one-loop multiplicative renormalization of various operators [2,3]. It is interesting to explore to what extent such methods lead to an improvement even in a sensitive case such as the one at hand. We find that our improved estimates compare quite well with Monte Carlo data also in this case.

The paper is organized as follows: In Sec. II we define the quantities which we set out to compute, and describe our calculation. In Sec. III we present our results and compare with Monte Carlo evaluations. In Sec. IV we obtain the improved estimates coming from cactus resummation.

II. FORMULATION OF THE PROBLEM

QCD with Wilson fermions on the lattice is described by the following action (see, e.g., Ref. [4] for standard notation and conventions):

$$S_L = \frac{1}{g_0^2} \sum_{x,\mu,\nu} \text{Tr} [1 - U_{\mu\nu}(x)] + \sum_{i=1}^{N_f} \sum_{x,y} \bar{\psi}_i(x) D(x,y) \psi_i(y) \quad (1)$$

$U_{\mu\nu}(x)$ is the standard product of link variables $U_{x,y}$ around a plaquette in the direction $\mu-\nu$, originating at point x , and $D(x,y)$ is given by:

$$D(x, y) = am_B \delta_{x,y} + \frac{1}{2} \sum_{\mu} [\gamma_{\mu} (U_{x,y} \delta_{x+\hat{\mu},y} - U_{x,y} \delta_{x,y+\hat{\mu}}) - r (U_{x,y} \delta_{x+\hat{\mu},y} - 2\delta_{x,y} + U_{x,y} \delta_{x,y+\hat{\mu}})] \quad (2)$$

As usual, g_0 denotes the bare coupling constant and a is the lattice spacing. The bare fermionic mass m_B must be set to zero for chiral invariance in the classical continuum limit.

The higher derivative term, multiplied by the Wilson coefficient r , breaks chiral invariance. It vanishes in the classical continuum limit; at the quantum level, it induces nonvanishing, flavor-independent corrections to the fermion masses.

Numerical simulation algorithms usually employ the hopping parameter,

$$\kappa \equiv \frac{1}{2 m_B a + 8 r} \quad (3)$$

as a tunable quantity. Its critical value, at which chiral symmetry is restored, is thus $1/8r$ classically, but gets shifted by quantum effects.

The renormalized mass can be calculated in textbook fashion from the fermion self-energy. Denoting by $\Sigma^L(p, m_B, g_0)$ the truncated, one particle irreducible fermionic two-point function, we have for the fermionic propagator:

$$\begin{aligned} S(p) &= \frac{1}{i \not{p} + m(p)} \sum_{k=0}^{\infty} \left(\Sigma^L(p, m_B, g_0) \frac{1}{i \not{p} + m(p)} \right)^k \\ &= \left[i \not{p} + m(p) - \Sigma^L(p, m_B, g_0) \right]^{-1} \end{aligned} \quad (4)$$

where : $\not{p} = \sum_{\mu} \gamma_{\mu} \frac{1}{a} \sin(ap^{\mu})$, $m(p) = m_B + \frac{2r}{a} \sum_{\mu} \sin^2(ap^{\mu}/2)$.

Requiring that the renormalized mass vanish, leads to:

$$S^{-1}(0) = 0 \quad \implies \quad m_B = \Sigma^L(0, m_B, g_0) \quad (5)$$

The above is a recursive equation for m_B , which can be solved order by order in perturbation theory.

We write the loop expansion of Σ^L as:

$$\Sigma^L(0, m_B, g_0) = g_0^2 \Sigma^{(1)} + g_0^4 \Sigma^{(2)} + \dots \quad (6)$$

Fig. I shows the two diagrams contributing to the 1-loop result $\Sigma^{(1)}$. The fermion mass involved in these diagrams must be set to its tree level value, $m_B \rightarrow 0$. The i^{th} diagram gives a contribution of the form $\frac{N^2-1}{N} c_i^{(1)}$, where $c_1^{(1)}, c_2^{(1)}$ are numerical constants.



FIGURE I. One-loop diagrams contributing to Σ^L . Wavy (solid) lines represent gluons (fermions).

A total of 26 diagrams contribute to the 2-loop quantity $\Sigma^{(2)}$, shown in Fig. II. Genuine 2-loop diagrams must again be evaluated at $m_B \rightarrow 0$; in addition, one must include to this order the 1-loop diagram containing an $\mathcal{O}(g_0^2)$ mass counterterm (diagram 23). The contribution of each diagram can be written in the form

$$(N^2 - 1)(c_{1,i}^{(2)} + \frac{c_{2,i}^{(2)}}{N^2} + \frac{N_f}{N} c_{3,i}^{(2)}) \quad (7)$$

where $c_{1,i}^{(2)}, c_{2,i}^{(2)}, c_{3,i}^{(2)}$ are numerical constants. Certain sets of diagrams, corresponding to renormalization of loop propagators, must be evaluated together in order to obtain an infrared-convergent result: these are diagrams 7+8+9+10+11, 12+13, 14+15+16+17+18, 19+20, 21+22+23.

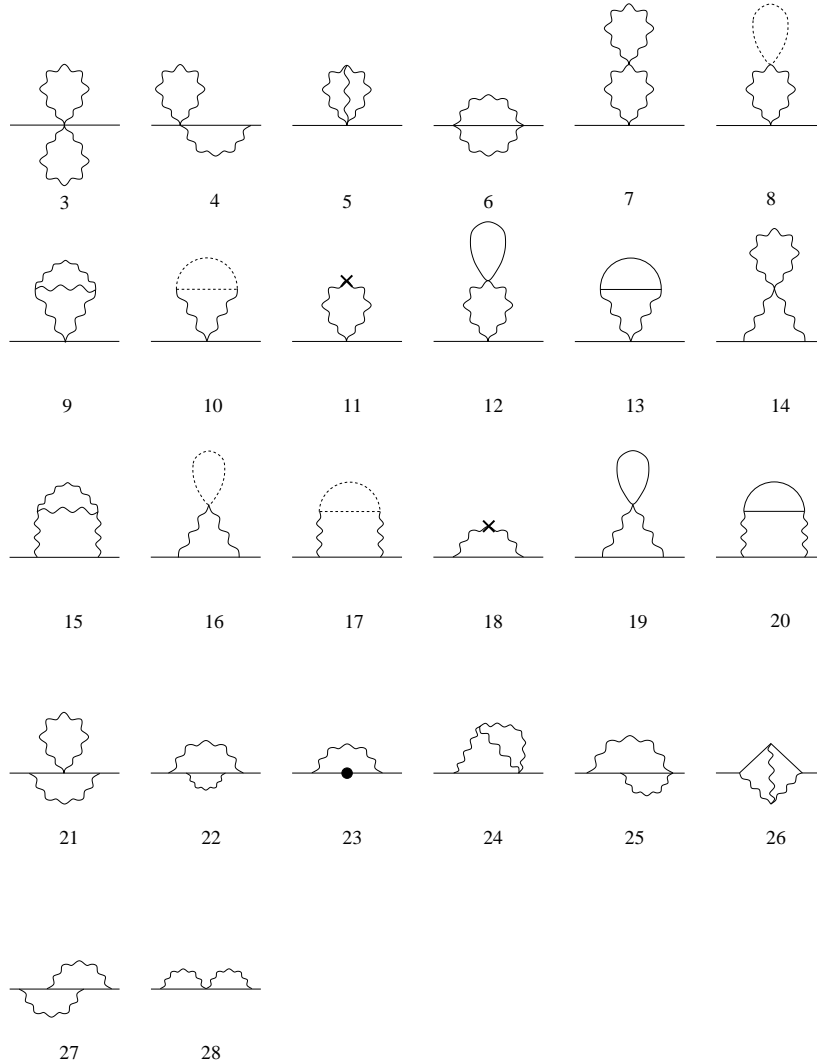


FIGURE II. Two-loop diagrams contributing to Σ^L . Wavy (solid, dotted) lines represent gluons (fermions, ghosts). Crosses denote vertices stemming from the measure part of the action; a solid circle is a fermion mass counterterm.

III. NUMERICAL RESULTS

The evaluation of the diagrams in this computation requires very extensive analytical work. To this end, we use a Mathematica package which we have developed for symbolic manipulations in lattice perturbation theory (see, e.g., Ref. [5]). Applied to the present case, this package allows us to perform in a rather straightforward way the following tasks: Contraction among the appropriate vertices; simplification of color/Dirac matrices; use of trigonometry and momentum symmetries for reduction to a more compact, canonical form; automatic generation of highly optimized Fortran code for the loop integration of each type of expression.

The integrals, typically consisting of a sum over a few hundred trigonometric products, are then performed numerically on lattices of varying finite size L . Our programs perform extrapolations of each expression to a broad spectrum of functional forms of the type: $\sum_{i,j} e_{ij} (\ln L)^j / L^i$, analyze the quality of each extrapolation using a variety of criteria and assign statistical weights to them, and finally produce a quite reliable estimate of the systematic error. Taking $L \leq 28$ leads to a sufficient number of significant digits in the results we present.

One important consistency check can be performed on those diagrams which are separately IR divergent; taken together in groups, as listed below Eq. (7), they give a finite and very stable extrapolation.

We present below the numerical values of the constants $c_i^{(1)}, c_{1,i}^{(2)}, c_{2,i}^{(2)}, c_{3,i}^{(2)}$. These constants depend only on the Wilson parameter r ; following common practice, we set $r = 1$.

Table I contains the contributions to the 1-loop quantity $\Sigma^{(1)}$. The total 1-loop result is

$$\Sigma^{(1)} = \frac{N^2 - 1}{N} (-0.162857058711(2)) \quad (8)$$

This result is known in the literature (see, e.g., Ref. [6], p. 246, and references contained therein).

The contributions to the 2-loop quantity $\Sigma^{(2)}$ are presented in table II. The total 2-loop result is

$$\Sigma^{(2)} = (N^2 - 1)(-0.017537(3) + \frac{1}{N^2} 0.016567(2) + \frac{N_f}{N} 0.00118618(8)) \quad (9)$$

In order to make a comparison with numerical simulations, let us set $N = 3$, $N_f = 2$ in the above; we obtain

$$\Sigma^{(1)}(N=3, N_f=2) = -0.434285489897(5) \quad (10)$$

$$\Sigma^{(2)}(N=3, N_f=2) = -0.11925(3) \quad (11)$$

In Table III we compare the final results for $m_c^{(1)} = g_0^2 \Sigma^{(1)}$ and $m_c^{(2)} = g_0^2 \Sigma^{(1)} + g_0^4 \Sigma^{(2)}$ with numerical simulation data at values of $\beta = 6/g_0^2$ equal to 5.6 [7] and 5.5 [8]. Also included in this table are the improved results obtained with the method described in the following Section. For easier reference, Table IV presents our results in terms of the critical hopping parameter $\kappa_c = 1/(2m_c a + 8r)$.

IV. IMPROVED PERTURBATION THEORY

In order to obtain improved estimates from lattice perturbation theory, one may perform a resummation to all orders of the so-called “cactus” diagrams [1–3]. Briefly stated, these are gauge-invariant tadpole diagrams which become disconnected if any one of their vertices is removed. The original motivation of this procedure is the well known observation of “tadpole dominance” in lattice perturbation theory. In the following we refer to Ref. [1] for definitions and analytical results.

Since the contribution of standard tadpole diagrams is not gauge invariant, the class of gauge invariant diagrams we are considering needs further specification. By the Baker-Campbell-Hausdorff (BCH) formula, the product of link variables along the perimeter of a plaquette can be written as

$$\begin{aligned}
 U_{x,\mu\nu} &= e^{ig_0 A_{x,\mu}} e^{ig_0 A_{x+\mu,\nu}} e^{-ig_0 A_{x+\nu,\mu}} e^{-ig_0 A_{x,\nu}} \\
 &= \exp \left\{ ig_0 (A_{x,\mu} + A_{x+\mu,\nu} - A_{x+\nu,\mu} - A_{x,\nu}) + \mathcal{O}(g_0^2) \right\} \\
 &= \exp \left\{ ig_0 F_{x,\mu\nu}^{(1)} + ig_0^2 F_{x,\mu\nu}^{(2)} + \mathcal{O}(g_0^4) \right\}
 \end{aligned}
 \tag{12}$$

The diagrams that we propose to resum to all orders are the cactus diagrams made of vertices containing $F_{x,\mu\nu}^{(1)}$. Terms of this type come from the pure gluon part of the lattice action. These diagrams dress the transverse gluon propagator P_A leading to an improved propagator $P_A^{(I)}$, which is a multiple of the bare transverse one:

$$P_A^{(I)} = \frac{P_A}{1 - w(g_0)},
 \tag{13}$$

where the factor $w(g_0)$ will depend on g_0 and N , but not on the momentum. The function $w(g_0)$ can be extracted by an appropriate algebraic equation that has been derived in Ref. [1] and that can be easily solved numerically; for $SU(3)$, $w(g_0)$ satisfies:

$$u e^{-u/3} \left[u^2/3 - 4u + 8 \right] = 2g_0^2, \quad u(g_0) \equiv \frac{g_0^2}{4(1 - w(g_0))}.
 \tag{14}$$

The vertices coming from the gluon part of the action, Eq. (1), get also dressed using a procedure similar to the one leading to Eq. (13) [1]. Vertices coming from the fermionic action stay unchanged, since their definition contains no plaquettes on which to apply the linear BCH formula.

One can apply the resummation of cactus diagrams to the calculation of additive and multiplicative renormalizations of lattice operators. Applied to a number of cases of interest [1,2], this procedure yields remarkable improvements when compared with the available nonperturbative estimates. As regards numerical comparison with other improvement schemes, such as boosted perturbation theory [9,10], cactus resummation fares equally well on all the cases studied [3].

One advantageous feature of cactus resummation, in comparison to other schemes of improved perturbation theory, is the possibility of systematically incorporating higher loop diagrams. The present calculation best exemplifies this feature, as we will now show.

Dressing the 1-loop result is quite straightforward: the fermionic propagator and vertices stay unchanged, and only the gluon propagator gets simply multiplied by $1/(1-w(g_0))$. The resulting values: $m_{c,\text{dressed}}^{(1)}$ and $\kappa_{c,\text{dressed}}^{(1)}$, are shown in Tables III and IV, respectively. It is worth noting that these values already fare better than the much more cumbersome undressed 2-loop results.

We now turn to dressing the 2-loop results. Here, one must take care to avoid double counting: A part of diagrams 7 and 14 has already been included in dressing the 1-loop result, and must be explicitly subtracted from $\Sigma^{(2)}$ before dressing. Fortunately, this part (we shall denote it by $\Sigma_{\text{sub}}^{(2)}$) is easy to identify, as it necessarily includes all of the $1/N^2$ part in $\Sigma^{(2)}$. A simple exercise in contraction of $SU(N)$ generators shows that $\Sigma_{\text{sub}}^{(2)}$ is proportional to $(2N^2 - 3)(N^2 - 1)/(3N^2)$. There follows immediately that:

$$\Sigma_{\text{sub}}^{(2)} = -0.016567(2N^2 - 3)(N^2 - 1)/(3N^2) \quad (15)$$

(cf. Eq. 9).

A further complication is presented by gluon vertices. While the 3-gluon vertex dresses by a mere factor of $(1-w(g_0))$, the dressed 4-gluon vertex contains a term which is not simply a multiple of its bare counterpart (see Appendix C of Ref. [1]). Once again, however, we are fortunate: this term must be dropped, being precisely the one which has already been taken into account in dressing the 1-loop result, while the remainder dresses in the same way as the 3-gluon vertex. In conclusion, cactus resummation applied to the 2-loop quantity $\Sigma^{(2)}$ leads to the following rather simple recipe:

$$m_{c,\text{dressed}}^{(2)} = \Sigma^{(1)} \frac{g_0^2}{1-w(g_0)} + (\Sigma^{(2)} - \Sigma_{\text{sub}}^{(2)}) \frac{g_0^4}{[1-w(g_0)]^2} \quad (16)$$

The end results, $m_{c,\text{dressed}}^{(2)}$ and $\kappa_{c,\text{dressed}}^{(2)}$, are included in Tables III and IV. Comparing with the Monte Carlo estimates, we see a definite improvement over non-dressed values. At the same time, a sizeable discrepancy still remains, as was expected from start. This discrepancy sets a benchmark for lattice perturbation theory; multiplicative renormalizations, calculated to the same order and improved by cactus dressing, are expected to be much closer to their exact values. We hope to return to these calculations in a future publication.

REFERENCES

- [1] H. Panagopoulos and E. Vicari, Phys. Rev. D 58 (1998) 114501.
- [2] H. Panagopoulos and E. Vicari, Phys. Rev. D 59 (1999) 057503.
- [3] H. Panagopoulos and E. Vicari, Nucl. Phys. B (PS) 83 (2000) 884.
- [4] H. J. Rothe, “Lattice Gauge Theories – An Introduction”, World Scientific (1992).
- [5] C. Christou, A. Feo, H. Panagopoulos, and E. Vicari, Nucl. Phys. B 525 (1998) 387.
- [6] I. Montvay, G. Münster, “Quantum Fields on a Lattice”, Cambridge U. Press (1994).
- [7] N. Eicker, P. Lacock, K. Schilling, A. Spitz, U. Glässner, S. Güsken, H. Hoerber, Th. Lipert, Th. Strickmann, P. Ueberholz, J. Viehoff, and G. Ritzenhöfer, Phys. Rev. D 59 (1999) 014509.
- [8] K. M. Bitar, R. G. Edwards, U. M. Heller, and A. D. Kennedy, Nucl. Phys. (PS) 53 (1997) 225-227.
- [9] G. Parisi, in: High-Energy Physics – 1980, XX Int. Conf., Madison (1980), ed. L. Durand and L. G. Pondrom (American Institute of Physics, New York, 1981).
- [10] G. P. Lepage and P. B. Mackenzie, Phys. Rev. D 48 (1993) 2250.

TABLE I. Coefficients $c_i^{(1)}$. $r = 1$.

i	$c_i^{(1)}$
1	-0.15493339023106
2	-0.007923668480(2)

TABLE II. Coefficients $c_{1,i}^{(2)}$, $c_{2,i}^{(2)}$, $c_{3,i}^{(2)}$. $r = 1$.

i	$c_{1,i}^{(2)}$	$c_{2,i}^{(2)}$	$c_{3,i}^{(2)}$
3	0.002000362950707492	-0.00030005444260612375	0
4	0.00040921361(1)	-0.00061382041(2)	0
5	0	0	0
6	-0.0000488891(8)	0.000097778(2)	0
7+8+9+10+11	-0.013927(3)	0.014525(2)	0
12+13	0	0	0.00079263(8)
14+15+16+17+18	-0.005753(1)	0.0058323(7)	0
19+20	0	0	0.000393556(7)
21+22+23	0.000096768(4)	-0.000096768(4)	0
24	0	0	0
25	0.00007762(1)	-0.00015524(3)	0
26	-0.00040000(5)	0	0
27	0	-0.000006522(1)	0
28	0.0000078482(5)	-0.000015696(1)	0

TABLE III. $m_c^{(1)}$ and $m_c^{(2)}$. $N = 3$, $N_f = 2$, $r = 1$.

	$\beta = 5.5$	$\beta = 5.6$
$m_c^{(1)}$	-0.473765988978(5)	-0.465305882032(5)
$m_c^{(2)}$	-0.61568(3)	-0.60219(3)
$m_{c,\text{dressed}}^{(1)}$	-0.658392964276(7)	-0.640695803036(7)
$m_{c,\text{dressed}}^{(2)}$	-0.76323(6)	-0.73997(6)
Simulation	-0.8975	-0.8446

TABLE IV. $\kappa_c^{(1)}$ and $\kappa_c^{(2)}$. $N = 3$, $N_f = 2$, $r = 1$.

	$\beta = 5.5$	$\beta = 5.6$
$\kappa_c^{(1)}$	0.1417943331149(4)	0.1414549557367(4)
$\kappa_c^{(2)}$	0.147740(3)	0.147154(3)
$\kappa_{c,\text{dressed}}^{(1)}$	0.1496286052353(6)	0.1488403462990(6)
$\kappa_{c,\text{dressed}}^{(2)}$	0.154475(6)	0.153373(6)
Simulation	0.16116(15)	0.158507 ⁺⁴¹ ₋₄₄